ELSEVIER

Biophysical Chemistry 113 (2005) 175–182

Biophysical Chemistry

www.elsevier.com/locate/bpc

Conformation of a synthetic antigenic peptide from HIV-1 p24 protein induced by ionic micelles

Patricia T. Campana[a], Leila M. Beltramini[a], Antonio J. Costa-Filho[a], Georgina Tonarelli[b], Javier Lottersberger[b], M. Lucia Bianconi[c,*]

[a]*Departamento de Física e Informática, Instituto de Física de São Carlos, C.P. 369, CEP 13566-970, São Carlos, Brazil*
[b]*Departamento de Química Orgánica, Facultad de Bioquímica y Cs. Biológicas, UNL, Ciudad Universitaria, C.C. 242, CP 3000, Santa Fe, Argentina*
[c]*Departamento de Bioquímica Médica, Instituto de Ciências Biológicas, UFRJ, Prédio do CCS, Bloco E, sala 38, Rio de Janeiro, RJ, CEP 21491-590, Brazil*

Received 30 July 2004; received in revised form 27 August 2004; accepted 27 August 2004
Available online 29 September 2004

Abstract

We studied the interaction of the peptide AAMQMLKETINEEAAEWDRVHPVHAGPIA from the HIV-1 p24 protein in the presence of SDS (anionic) and CTABr (cationic) micelles at pH 7.0 by circular dichroism, fluorescence, and electron spin resonance (ESR). The micelles induced secondary structure as well as a blue shift in the tryptophan fluorescence emission, indicating an interaction between the peptide and the micelles. However, different contents of secondary structure elements were found when the peptide interacts with SDS or CTABr micelles. Steady-state anisotropy indicates a constraint on the rotational mobility of the tryptophan residue of the peptide upon interaction with micelles. ESR studies pointed to different locations for the peptide in either micelle. Our results suggested that at least part of the peptide might be located at the hydrophobic core of the CTABr micelles, probably at the C-terminal region, while it is more inserted into the SDS micelles.
© 2004 Elsevier B.V. All rights reserved.

Keywords: p24 HIV-1 peptide; SDS micelles; CTABr micelles; Circular dichroism fluorescence; ESR

1. Introduction

Recent discussions about initial infection and virus dissemination processes involving HIV-1 virus have focused on proteins from the viral envelope [1]. Although they play a key role in viral infection, it has been shown that proteins from the inner core of the HIV-1 are also involved in relevant processes such as assembly or disassembly of the capsid protein, maturation, and life cycle of the virus [2,3]. Capsid assembly, in turn, is crucial for viral infectivity as shown for HIV-1 p24 protein [4] and for hepatitis B virus [5]. The interactions between viral proteins and host cells are generally affected by biomolecules incorporated in the phospholipid framework of the membrane, which can be studied directly in vivo and indirectly in vitro using biomimetic models such as vesicles (multilamellar and unilamellar) and micelles [6–8].

The proteins from the capsid and matrix of HIV-1, p24 and p17, are also important in diagnosing and in monitoring the infection since antibodies against p24 have been detected in the plasma of infected patients [9]. However, how the host-cell defense system recognizes these proteins is still the object of speculation [10].

The most relevant capsid protein, p24, plays a structural role in both the expression and in the mature forms of the gag gene [11]. This protein consists of two alpha helical domains: the N-terminal (seven α-helices) and the C-terminal (four α-helices) interconnected by a flexible linker

Abbreviations: HIV-1, human immunodeficiency virus, type 1; CD, circular dichroism; ESR, electron spin resonance; Fmoc, 9-fluorenylmethoxycarbonyl; SDS, sodium dodecylsulfate; CTABr, hexadecyltrimethylammonium bromide; PBA, sodium phosphate, boric acid, sodium acetate buffer; cmc, critical micelle concentration; CAT-16, 4-(*N*,*N*-dimethyl-*N*-hexadecyl) ammonium-2,2,6,6-tetramethylpiperidine-1-oxyl iodide; 5-SASL, 5-doxyl stearic acid; 12-SASL, 12-doxyl stearic acid.

* Corresponding author. Tel.: +55 21 2562 6760; fax: +55 21 2270 1635.
E-mail address: bianconi@bioqmed.ufrj.br (M.L. Bianconi).

0301-4622/$ - see front matter © 2004 Elsevier B.V. All rights reserved.
doi:10.1016/j.bpc.2004.08.006

[12]. Mutations and deletions within the C-terminal domain generally impair or abolish viral assembly, whereas mutations on the amino-terminal core domain often give rise to viruses that can assemble and bud, but are non-infectious and typically do not form a normal capsid [13]. Capsid assembly is crucial for viral infectivity [11]; consequently, the use of peptides from p24 is a promising approach for structural studies towards understanding the life cycle of the virus as well as elucidating the viral transfection mechanism. This approach has been applied in studies of synthetic peptides derived from specific protein sequences. The main goals were to investigate the role of peptide sequences in protein structure, their interaction with biomimetic systems, and their involvement in several biological processes such as immune response analysis, bioaffinity, inhibition of cell adhesion and binding to infectious elements.

In the analysis of synthetic peptides containing minimal size epitopes from HIV-1 p24 protein derived from the gag gene product, Tonarelli et al. [14] showed that the antibody recognition may be improved by adding more residues at the N- and C-terminal ends of the peptide. This strategy can also introduce structural elements in the polypeptide chain in order to constrain its flexibility. The tendency to form secondary structures has been observed for some immunogenic and antigenic peptides [15,16], and long peptides (15 or more residues) may indeed mimic the natural conformations [17,18]. On the other hand, when free peptides bind to structured molecular complexes, these interactions can promote structural changes in both the peptide and the molecular complex. In this sense, the interactions of peptides with biomimetic systems can be the first step to understanding the mechanisms underlying the peptide–macromolecular assemblies interactions. One kind of structured molecular complex largely used as a biomimetic system has been the micelles of ionic surfactants. Despite the inherent simplifications of this model, micelles are also of interest in biological systems, owing to the similarity between the micellar core and cell membrane interior [19].

We investigated micelle-induced conformational changes on a p24-1 peptide (sequence AAMQMLKETINEEAAEWDRVHPVHAGPIA), initially obtained from the gag gene product [9], which corresponds to the region 64–92 in the N-terminal domain of p24 HIV-1 protein [20]. The peptide–micelle interactions were studied by circular dichroism (CD), fluorescence and electron spin resonance (ESR), and the results were used to build up a structural model for the docking of the peptide on the biomimetic system.

2. Experimental

2.1. Peptide synthesis

A peptide corresponding to the sequence 64–92 of the p24 HIV-1 was synthesized as C-terminal carboxamides by solid phase with the 9-fluorenyl-methoxycarbonyl (Fmoc) strategy, and purified according to Tonarelli et al. [14]. The peptide solution was prepared from a stock of 1 mg/l in water and final concentrations of dilutions were corrected using the optical density (at 280 nm) and molar extinction coefficient (1.769 M^{-1} cm^{-1}) estimated from its amino acid composition according to Gill and von Hippel [21].

2.2. Micelle preparation

The solutions of hexadecyltrimethylammonium bromide (CTABr) and sodium dodecylsulfate (SDS) were prepared in 10 mM sodium phosphate, boric acid, sodium acetate buffer (PBA), pH 7.0. The critical micelle concentration (cmc) of these surfactants was determined by isothermal titration calorimetry according to Paula et al. [22] by using a MCS-ITC calorimeter from MicroCal (Northampton, MA). In the conditions used here (PBA buffer at 25 °C), the cmc values were 2.4 mM for SDS and 0.35 mM for CTABr (data not shown). In order to have either monomers or micelles in solution the final concentrations of surfactants used were, respectively, 0.5 and 8.0 mM of SDS, and 0.01 and 1.0 mM for CTABr. The micelles were also prepared with 1 mol% of the following spin labels: 4-(*N*,*N*-dimethyl-*N*-hexadecyl) ammonium-2,2,6,6-tetramethylpiperidine-1-oxyl iodide (CAT-16), 5-doxyl stearic acid (5-SASL) or 12-doxyl stearic acid (12-SASL). Incorporation of spin labels was done by adding the desired amount of detergent solution to a film obtained after drying the stock chloroform solution of the spin label in speed-vac for 10 min, followed by vortexing and 30 min incubation at room temperature. The surfactants and spin labels were purchased from Sigma (St. Louis, MO, USA) and used without further purification.

2.3. Far-UV circular dichroism and secondary structure content

Far-UV CD spectra (190–250 nm) were recorded at 25 °C in a Jasco J715 (Jasco, Japan) using a cylindrical quartz cells (1 mm path length), with 53 μM p24-1 in PBA, either in the absence or in the presence of surfactants. The spectra were recorded after accumulation of 16 runs. The CD spectra of surfactant solutions were subtracted to eliminate background effects due to monomers or micelles. Quantitative prediction of the secondary structure was performed by deconvolution of the CD spectra using the Selcon program [23], developed by Sreerama et al. [24], with a root mean square (RMS) lower than 1% for all deconvolutions.

2.4. Steady-state fluorescence

Steady-state fluorescence spectra (295–450 nm) of 25 μM p24-1 in PBA were obtained at 25 °C in ISS K2 spectrofluorimeter (ISS, Illinois, USA) using rectangular quartz cuvettes (1 cm path length) and at optical density less than 0.07–0.08 to avoid inner filter effects. The interaction

with micelles was studied by the changes in tryptophan fluorescence of the peptide with excitation at 280 nm. The fluorescence spectra of detergent solutions were subtracted to eliminate scattering due to micelles.

2.5. Steady-state anisotropy

Anisotropy measurements were carried out at 25 °C in 1 cm path length quartz cuvettes with L-format. The same samples measured in fluorescence experiments were used and excitation occurred at 280 nm. Anisotropy values (r) were calculated according to Lakowicz [25]: $r = \frac{I_{\parallel} - I_{\perp}}{I_{\parallel} + 2I_{\perp}}$, where $I_{\parallel}$ and $I_{\perp}$ are the parallel and the perpendicular components.

In order to eliminate the background, $I_{\parallel}$ and $I_{\perp}$ of the buffer and micelles were measured and subtracted from those of the peptide solutions.

2.6. ESR experiments and simulations

Room temperature ESR measurements were performed with a Varian E-109 spectrometer. Each sample (1.50 mM of p24-1 in CTABr or 0.4 mM of p24-1 in SDS micelles) was drawn into a quartz flat-cell, which was in turn placed in the rectangular cavity. A field-modulation of 1.0 G and microwave power of 10 mW were used. The spectra were collected over a range of 100 G.

The ESR spectra were simulated by means of a non-linear least-squares program developed by Freed et al. [26–28]. This program is based on the stochastic Liouville equation and allows the quantitative characterization of the dynamic structure of vesicles. The dynamics of the model system is characterized by the rotational diffusion rate ($R_{\perp}$) of the nitroxide radical around an axis perpendicular to the mean symmetry axis for the rotation. This symmetry axis is also the direction of preferential orientation of the spin label moiety [27]. For chain labels (5-SASL and 12-SASL), $R_{\perp}$ accounts for the wagging motion of the long axis of the stearic acid chain. For the label CAT-16, it represents the wagging motion of the headgroup region. The hyperfine and g-tensors components used in the simulations were obtained from Ge et al. [29].

3. Results and discussion

3.1. Secondary structure

The CD results showed that p24-1 adopts a random structure in buffer only as expected for a small peptide in solution. The deconvolution of the p24-1 spectrum in buffer confirmed the high content of unordered structure (94%), consistent with the CD minimum at 200 nm (Fig. 1). This large content of unordered structure required the use of a special reference set of 48 proteins, which included spectra from denaturated proteins for deconvolution [30].

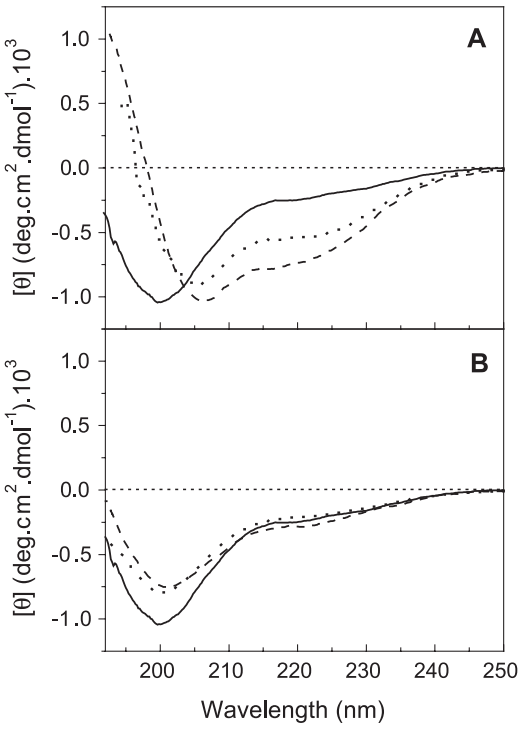

Fig. 1. CD spectra of p24-1 in buffer (solid), SDS (dashed) and CTABr (dotted) solutions at concentration above (A) and below (B) the cmc. The final concentrations were 8 and 1 mM for micellar, and 0.5 and 0.01 mM for monomeric solutions (SDS and CTABr, respectively), and 0.05 mM for p24-1, in 10 mM PBA buffer, pH 7.0.

The addition of SDS or CTABr micelles induced folded secondary structure in p24-1 (Fig. 1A). The CD spectrum of p24-1 in SDS micelles showed two negative minima, one at 206 nm and a weaker one at about 220 nm, with a maximum at 191 nm, mainly associated to the transitions found in helical structures [31]. Similar CD spectrum was observed in the presence of CTABr micelles. The CD spectra were deconvoluted with a reference set of 33 proteins [32], which was adequate to achieve the convergence of the results. SDS and CTABr micelles were able to stabilize the p24-1 secondary structure, leading to helical structure contents of 23% for SDS- and 13% for CTABr-bound peptide. The induction of beta structure fractions by either micelle was somewhat different (20% in SDS, and 26% in CTABr), while the unordered fractions were similar in both cases (54% in SDS, and 58% in CTABr).

Since above the cmc, micelles and monomers co-exist in solution, we also checked the effects of monomeric surfactants in the CD spectrum of p24-1 (Fig. 1B). In this case, the p24-1 CD spectra were essentially the same as that in buffer (Fig. 1B). Thus, monomers only were not able to stabilize a secondary structure in p24-1 showing that the macromolecular assembly is important to inducing secondary structure. The differences in the intensity (about 20%) observed in the CD spectra of p24-1 in the absence and in the presence of monomeric CTABr and SDS are probably due to scattering effects [33].

The helical contribution on micelle-bound p24-1 secondary structure is only about 20% in SDS micelles, in contrast to what is usually observed for some other peptides [34], where it may correspond to ca. 60% of the total secondary structure content. In the case of CTABr micelles, the secondary structure of the peptide is probably more extended due to the higher beta content, suggesting that micelles with different charges in the headgroups stabilize different conformations. The helical structure content is probably the result of a conformational change in residues within segments 1 to 18. This supposition is based on results from two secondary structure prediction programs. The first, based on computation neural networks that consider the secondary structure of a particular residue to be a function of the residue and its environment, named GOR4 [35], predicted about 38% of helical structure between residues 7 and 17. The second, NNPREDICT [36], calculates the secondary structure for each residue in an amino acid sequence, and showed about 50% of helical between the residues 3–8 and 9–18. Therefore, upon interaction with the micelles, the N-terminal region of the peptide is most likely to be assuming a helical structure. In addition, the two Pro residues, which are rarely present in helical forms [37], found in the C-terminus suggest that the 20–29 segment on the peptide is probably forming loops or unordered structures.

3.2. Steady-state fluorescence spectrum and anisotropy

The effect of SDS and CTABr in the monomeric and micellar states on the fluorescence spectra of p24-1 can be seen in Fig. 2. The p24-1 has a single Trp residue in the sequence at position 17. The emission maximum (λ_{max}^{emiss}) of p24-1 in buffer is 350 nm, which is consistent with the exposition of the tryptophan residue in the aqueous medium. However, when the peptide interacts with SDS or CTABr micelles there is a blue shift of the tryptophan emission spectrum, decreasing to 338 and 339 nm in SDS and CTABr micelles, respectively. A significant increase in the fluorescence intensity was also observed for the samples containing CTABr micelles and p24-1, indicating a transfer of the tryptophan moiety from an exposed environment (the aqueous phase) to a partially buried environment within the micelles [38]. It has been proposed that the tryptophan indole ring in SDS micelles is localized near or at the micelle/water interface [39]. Additionally, the Trp-17 blue shift found in SDS micelles is not as intense as than that observed for a Trp residue located at the center of a bilayer [40], and for a peptide in the SDS micelle/water interface [41]. This indicates that the Trp-17 is not deeply inserted, but still localized in the hydrophobic core close to the headgroup region. This discussion could be extended to CTABr micelles, in which case, the blue shift was similar to SDS.

In addition, for CTABr micelles, there was a significant increase of the Trp fluorescence intensity as shown in Fig. 2A. This evidence suggests that different local conformations in p24-1 structure are induced by either micelle as already found by CD. The peptide interaction with CTABr micelles indicates an annulment of a quenching effect by the side chains of p24-1 most likely from Glu-16 and Asp-18 neighboring residues [42]. It is possible that in CTABr micelles the Trp fluorescence is not suppressed by the natural quenchers due to a conformational change. In contrast, there is no significant change in the fluorescence intensity of p24-1 in SDS micelles although a conformational change was observed by CD (Fig. 1A). In this case, the Trp residue probably remains quenched by the acidic side chains, thus having similar intensity to that observed for the peptide in buffer. The location of those moderated quenchers in p24-1 sequence (Glu-16 and Asp-18) strongly supports the hypothesis of internal suppression effect that will cause or not the quenching of the Trp-17 fluorescence depending on the conformational state induced by either micelle.

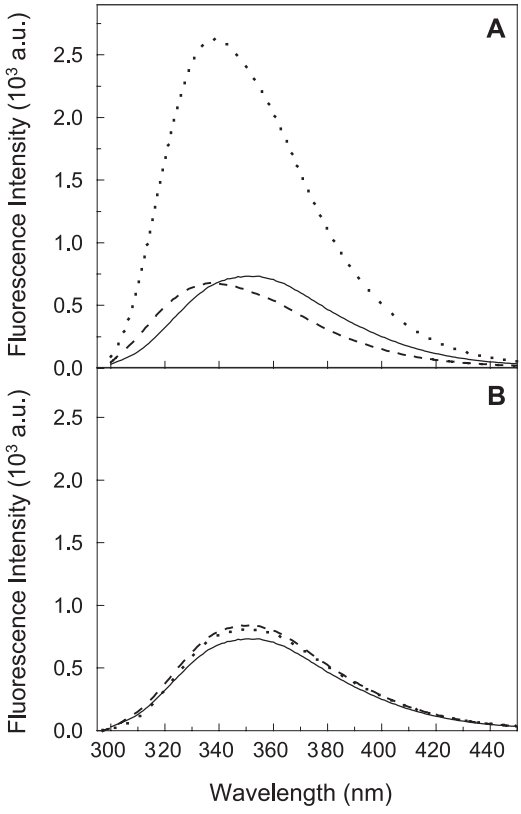

Fig. 2. Fluorescence spectra of p24-1 in buffer (solid) or in the presence of SDS (dashed) or CTABr (dotted) solutions in concentrations above (A) and below (B) the cmc. The excitation wavelength was 280 nm, and the emission was scanned from 300 to 450. The final concentrations were 8 and 0.5 mM for micellar and monomeric SDS, 1 and 0.01 mM for micellar and monomeric CTABr. Peptide concentration was 0.05 mM in 10 mM PBA buffer, pH 7.0.

In agreement with the CD studies, the p24-1 spectra with monomeric surfactants (Fig. 2B) were very similar to that observed in buffer, showing that p24-1 only interacts with the surfactant in the micellar state.

Table 1 shows the fluorescence anisotropy values for p24-1 in buffer only and in the presence of micelles. The

anisotropy of p24-1 in buffer indicates the maximum rotational freedom of molecular motion for the Trp residue in this peptide. Addition of SDS micelles caused an increase in the anisotropy indicating constraint on the rotational mobility of this residue, which corroborates with the previous findings of its insertion into the micelles. However, the increase in anisotropy observed with CTABr micelles was markedly higher than that in SDS micelles suggesting that the Trp-17 residue is in an environment of more restricted rotational motion.

3.3. Electron spin resonance

In order to obtain information on the location of the peptide in the micelles, we carried out ESR experiments using spin labels with the nitroxide group at different positions along the stearic acid chain (CAT-16, 5-SASL, and 12-SASL). The labels were incorporated into SDS and CTABr micelles and the spectra are shown in Figs. 3 and 4, respectively. The relative polarity of the spin label environment can be related to the isotropic hyperfine splitting constant (a_0), which is calculated as one-half the difference in the resonance field of the high- and low-field lines.

Table 2A shows the dependence of a_0 on nitroxide position inside the micelles. The CAT-16 nitroxide group is located at the headgroup region of the micelles and exhibits relatively high values for a_0 in both SDS and CTABr, close to those found for a similar spin label in SDS micelles [43]. As expected for the other two spin labels, where the nitroxide group is located down the stearic acid chain, a_0 values indicate a decreased polarity inside the micelles. The addition of p24-1 to SDS micelles does not change a_0 at the polar headgroup but causes a decrease in polarity at n=5 and n=12 positions (Table 2A). On the other hand, the peptide causes a decrease in polarity at the polar headgroup and n=12 position when added to CTABr micelles, without a significant change in the polarity of the n=5 environment.

Table 2B presents the best-fit rotational diffusion rates ($R_\perp$) obtained from NLLS simulations. In the presence of p24-1, the $R_\perp$ values in SDS micelles are reduced by a factor of 1.2, 1.5, and 2.1 for CAT-16, 5-SASL and 12-SASL, respectively. Hence, motion becomes more hindered as the label locates deeper in the SDS micelles upon peptide binding. As for the CTABr micelles, the effect of the peptide on the $R_\perp$ values is most pronounced in the headgroup region, where the motion is slowed down by a factor of ca. 3.

The dynamics of the surfactant chains in SDS and CTABr micelles are somehow affected in different ways in the presence of the peptide p24-1. The fluidity of SDS micelles is progressively decreased from the headgroup down to the n=12 position, whereas in CTABr it is observed a severe reduction in mobility at the headgroup region. The ESR results thus suggest that the peptide interacts differently with cationic and anionic micelles, most likely adopting a distinct conformation in each case, which is in agreement with the above results from CD and fluorescence spectroscopy.

Table 1
Steady-state anisotropy values for p24-1 fluorescence at pH 7.0

Condition	Anisotropy (r^s)
Buffer only	0.028±0.004
With SDS micelles	0.039±0.005
With CTABr micelles	0.062±0.002

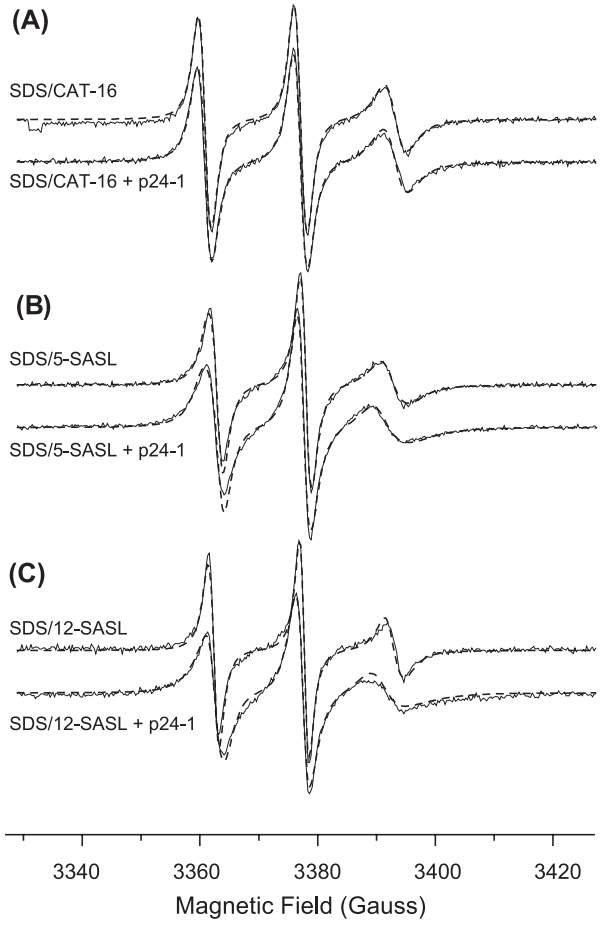

Fig. 3. ESR spectra of CAT-16 (A), 5-SASL (B) and 12-SASL (C) in SDS micelles in the absence and in the presence of 0.4 mM p24-1 in 10 mM PBA buffer, pH 7.0. The final concentration of SDS was 8 mM, containing 1 mol% of each spin label. Solid lines: experimental spectra; dashed lines: calculated spectra obtained by NLLS simulations.

3.4. Concluding remarks

The CD, ESR, and fluorescence experiments in samples containing p24-1 peptide and micelles (SDS and CTABr) revealed significant interactions between them. Different contents of secondary structure were induced by either micelle: a lower helical content is observed with CTABr upon micelle/peptide interaction. As a consequence, in this system the p24-1 shows a higher content of beta structures as compared to the SDS micelles.

The steady-state fluorescence experiments suggest that the Trp residue is located at the Stern layer of either

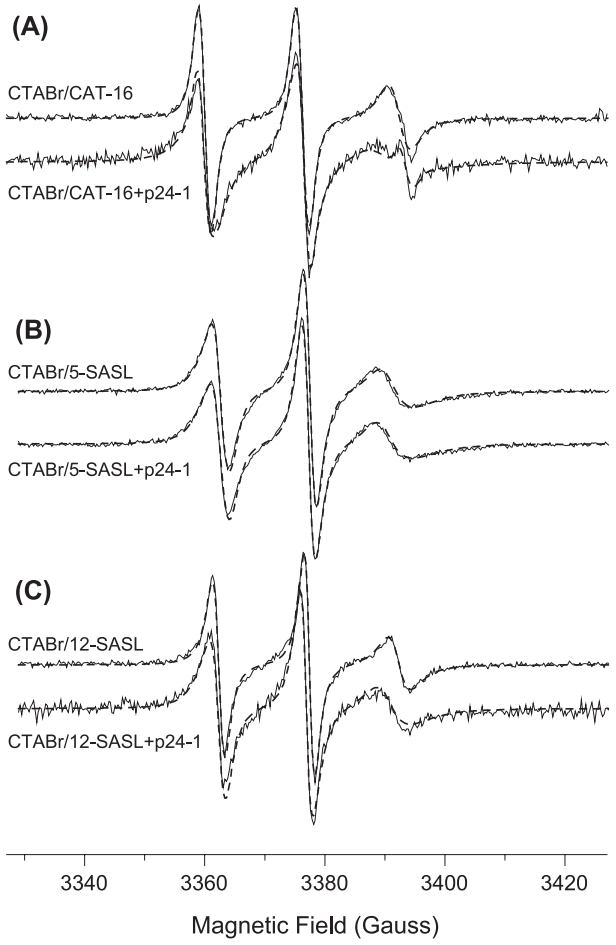

Fig. 4. ESR spectra of CAT-16 (A), 5-SASL (B) and 12-SASL (C) in CTABr micelles in the absence and in the presence of 1.5 mM p24-1 in 10 mM PBA buffer, pH 7.0. The final concentration of CTABr was 1 mM, containing 1 mol% of each spin label. Solid lines: experimental spectra; dashed lines: calculated spectra obtained by NLLS simulations.

micelle. Changes in Trp fluorescence are widely used since this chromophore is very sensitive to the polarity of the environment, being characterized by an emission maximum between 355 and 308 nm as the polarity decreases. In aqueous medium, the Trp-17 seems to be highly dynamic due to lack of structure in the peptide, with the emission maximum at 350 nm. The 11–12 nm blue-shift on Trp-17 fluorescence indicates that this portion of the peptide is located in a more hydrophobic environment upon interaction with the micelles. This blue shift is similar to that observed by Hsu et al. [44] for the interaction of a 20-amino acid fusion peptide from Influenza virus Hemagglutinin with SDS micelles. However, it is indicative that the Trp-17 from p24-1 is not located in the core of the micelles since in lipid membranes tryptophan-containing peptides show an emission maximum around 318–320 nm. Therefore, the Stern layer, which contains not only the hydrophilic headgroups and water molecules but also some hydrophobic domains from the surfactant tails, is the probable location for the Trp-17. It is interesting to note that although a similar red-shift was observed, the Trp residue is in an environment of more restricted rotational motion in the case of CTABr. Furthermore, with CTABr micelles the Trp-17 fluorescence intensity increases, probably because it is not suppressed by the natural quenchers closely located in the sequence (Glu-16 and Asp-18). This is not observed with SDS micelles, suggesting that this region of the p24-1 is in a different conformation when interacting with either micelle. It is also possible that these natural quenchers are neutralized by electrostatic interactions with the positive charges at the CTABr polar headgroups. This, however, does not explain why the red-shift in the emission maximum is similar with both micelles since SDS presents negatively charged headgroups which could cause a repulsion of the Glu-16 and the Asp-18, although the proximity to the headgroups can cause a change in the apparent pK_a of either residue. The fact that the ESR experiments show that the peptide interacts with the core as well as with the polar headgroups of the surfactants in CTABr micelles while it seems to be more inserted into the SDS micelles, suggests that the p24-1 is in a more extended conformation in CTABr than in SDS micelles. This hypothesis is corroborated by the CD experiments since in CTABr micelles p24-1 presents a higher content of beta structures that are more extended than alpha-helix.

The hydrophobic sequence in the C-terminus (VHP VHAGPIA) suggests that this end of the peptide is more inserted in the core of the micelles. The interaction between this portion of the peptide and the micelles may be causing the different rearrangement of the peptide in each micelle, favoring the stabilization of an unordered structure. This suggestion is not only based on our results but also on those from Dixon et al. [45], where the addition of isoleucine residues to the C- and N-terminal ends of a short peptide (IICNNPHII) from an antibody-binding region of hemagglutinin A promoted the interaction with detergent micelles, and stabilized the formation of a type I/III hairpin turn.

Table 2
Isotropic hyperfine values a_0 measured as one-half the distance between the low- and high-field lines in the ESR spectra along with the best-fit parameters of $R_\perp$ from NLLS analysis for ESR spectra of CAT-16, 5-SASL, and 12-SASL in pure surfactant micelles and peptide-containing micelles

Parameter	Spin-label	SDS micelles		CTABr micelles	
		Only	+p24-1	Only	+p24-1
(A) a_0 (Gauss)	CAT-16	16.3	16.3	16.0	15.5
	5-SASL	15.1	14.7	14.5	14.3
	12-SASL	15.5	14.7	15.0	14.5
(B) $R_\perp$ (10^8 s^{-1})	CAT-16	2.09	1.82	2.40	0.78
	5-SASL	1.45	0.94	1.05	1.01
	12-SASL	2.23	1.06	1.61	0.95

The least-squares estimated errors in $R_\perp$ is ±5%.

Acknowledgments

The authors are grateful to FAPESP, FAPERJ and CNPq (Brazil) for the financial support.

References

[1] D.M. Eckert, P.S. Kim, Mechanisms of viral membrane fusion and its inhibition, Ann. Rev. Biochem. 70 (2001) 777–810.
[2] B.G. Turner, M.F. Summers, Structural biology of HIV, J. Mol. Biol. 285 (1999) 1–32.
[3] C. Tang, E. Loeliger, I. Kinde, S. Kyere, K. Mayo, E. Barklis, Y.N. Sun, M.J. Huang, M.F. Summers, Antiviral inhibition of the HIV-1 capsid protein, J. Mol. Biol. 327 (5) (2003) 1013–1020.
[4] B.M. Forshey, U. von Schwedler, W.I. Sundquist, C. Aiken, Formation of a human immunodeficiency virus type 1 core of optimal stability is crucial for viral replication, J. Virol. 76 (11) (2002) 5667–5677.
[5] K. Deres, C.H. Schroder, A. Paessens, S. Goldmann, H.J. Hacker, O. Weber, T. Kramer, U. Niewohner, U. Pleiss, J. Stoltefuss, E. Graef, D. Koletzki, R.N.A. Masantschek, A. Reimann, R. Jaeger, R. Gross, B. Beckermann, K.H. Schlemmer, D. Haebich, H. Rübsamen-Waigmann, Inhibition of hepatitis B virus replication by drug-induced depletion of nucleocapsids, Rubsamen–Waigmann, 299 (5608), Science (2003) 893–896.
[6] K. Gawrisch, K.-H. Han, J-.S. Yang, L.D. Bergelson, J.A. Ferretti, Interaction of peptide fragment 828–848 of the envelope glycoprotein of Human Immunodeficiency Virus type 1 with lipid bilayers, Biochemistry 32 (1993) 3112–3118.
[7] J.J. Chou, J.D. Kaufman, S.J. Stahl, P.T. Wingfield, A. Bax, Micelle-induced curvature in a water-insoluble HIV-1 Env peptide revealed by NMR dipolar coupling measurement in stretched polyacrylamide gel, J. Am. Chem. Soc. 124 (2002) 2450–2451.
[8] D. Trommeshauser, H.J. Galla, Interaction of a basic amphipatic peptide from the carboxyterminal part of the HIV envelope protein gp41 with negatively charged lipid surfaces, Chem. Phys. Lipids 94 (1998) 81–96.
[9] A.R.M. Coates, J. Cookson, G.J. Barton, M.J. Zvelebil, M.J.E. Sternberg, AIDS vaccine predictions, Nature 326 (1987) 549–550.
[10] H.R. Gelderblom, E.H.S. Hausmann, M. Ozel, G. Pauli, M.A. Koch, Fine-structure of human-immunodeficiency-virus (HIV) and immunolocalization of structural proteins, Virology 156 (1987) 171–176.
[11] A. Cimarelli, J.-L. Darlix, Assembling the human immunodeficiency virus type 1, Cell. Mol. Life Sci. 59 (2002) 1166–1184.
[12] H. Dobeli, H. Andres, N. Breyer, N. Draeger, D. Sizmann, M.T. Zuber, B. Weinert, B. Wipf, Recombinant fusion proteins for the industrial production of disulfide bridge containing peptides: purification, oxidation without concatamer formation, and selective cleavage, Protein Expr. Purif. 12 (1998) 404–414.
[13] T. Dorfman, A. Bukovsky, A. Öhagen, S. Höglund, H.G. Göttlinger, Functional domains of the capsid protein of HIV-1, J. Virol. 68 (1994) 8180–8187.
[14] G. Tonarelli, J. Lottersberger, J.L. Salvetti, S. Jacchieri, R.A. Silva-Lucca, L.M. Beltramini, Secondary structure-improved bio-affinity correlation in elongated and modified synthetic epitope peptides from p24 HIV-1 core protein, Lett. Pept. Sci. 7 (4) (2000) 217–224.
[15] H.J. Dyson, K.J. Cross, E.A. Houghten, I.A. Wilson, P.E. Wrigth, R.A. Lerner, The immunodominant site of a synthetic immunogen has a conformational preference in water for a type-II reverse turn, Nature 318 (1985) 480–483.
[16] H.J. Dyson, P.E. Wrigth, Antigenic peptides, FASEB J. 9 (1995) 37–42.
[17] P. Leinikki, M. Lehtinen, H. Hyoty, P. Parkkonen, M.L. Kantanen, J. Hakiñomem, Synthetic peptides as diagnostic-tools in virology, Adv. Virus Res. 42 (1993) 149–186.
[18] E. Benjamini, M. Shimizu, J. Young, C. Leung, Immunochemical studies on tobacco mosaic virus protein. 6: characterization of antibody populations following immunization with tobacco mosaic virus protein, Biochemistry 7 (1968) 1253–1257.
[19] M.F. Emerson, A. Holtzer, Hydrophobic bond in micelar systems effects of various additives on stability of micelles of sodium dodecyl sulfate and of *N*-dodecyltrimethylammonium bromide, J. Phys. Chem. 71 (10) (1967) 3320–3329.
[20] C. Berthet-Colominas, S. Monaco, A. Novelli, G. Sibai, F. Mallet, S. Cusak, Head-to-tail dimers and interdomains flexibility revealed by the crystal structure of HIV-1 capsid protein (p24) complexed with a monoclonal antibody Fab, EMBO J. 18 (1999) 1124–1136.
[21] S.C. Gill, P.H. von Hippel, Calculation of protein extinction coefficients from amino acid sequence data, Anal. Biochem. 182 (1989) 319–326.
[22] S. Paula, W. Süs, J. Tuchtenhagen, A. Blume, J. Phys. Chem. 99 (1995) 11742–11751.
[23] N. Sreerama, R.W. Woody, A self-consistent method for the analysis of protein secondary structure from circular-dichroism, Anal. Biochem. 209 (1993) 32–44.
[24] N. Sreerama, S.Y. Venyaminov, R.W. Woody, Estimation of the number of alpha-helical and beta-strand segments in proteins using circular dichroism spectroscopy, Protein Sci. 8 (1999) 370–380.
[25] J.R. Lakowicz, Principles of Fluorescence Spectroscopy, Plenum Press, New York, 1983, pp. 112–150.
[26] E. Meirovitch, A. Nayeem, J.H. Freed, Analysis if protein–lipid interactions based on model simulations of electron spin resonance spectra, J. Phys. Chem. 88 (1984) 3454–3465.
[27] D.J. Schneider, J.H. Freed, Calculating slow motional magnetic resonance spectra: a user's guide, in: L.J. Berliner, J. Reuben (Eds.), Spin Labeling Theory and Applications, vol. 8, Plenum Press, New York, 1989, pp. 1–76.
[28] D.E. Budil, S. Lee, S. Saxena, J.H. Freed, Nonlinear-least-squares analysis of slow-motion EPR spectra in one and two dimensions using a modified Levenberg–Marquardt algorithm, J. Magn. Reson., A 120 (1996) 155–189.
[29] M. Ge, S.B. Rananavare, J.H. Freed, ESR studies of stearic acid binding to bovine serum albumin, Biochim. Biophys. Acta 1036 (1990) 228–236.
[30] N. Sreerama, S.Y. Venyaminov, R.W. Woody, Estimation of protein secondary structure from circular dichroism spectra: inclusion of denatured proteins with native proteins in the analysis, Anal. Biochem. 287 (2000) 243–251.
[31] R. Woody, N. Berova, K. Nakanishi, Circular Dichroism: Principles Applications, VCH Publishers, New York, 1994.
[32] N. Sreerama, R.W. Woody, Estimation of protein secondary structure from circular dichroism spectra: Comparison of CONTIN, SELCON, and CDSSTR methods with an expanded reference set, Anal. Biochem. 282 (2000) 252–260.
[33] A.S. Ladokhin, S. Jayasinghe, S.H. White, How to measure and analyze tryptophan fluorescence in membranes properly, and why bother? Anal. Biochem. 285 (2000) 235–245.
[34] D.K. Chang, S.F. Cheng, W.J. Chien, The amino-terminal fusion domain peptide of human immunodeficiency virus type 1 gp41 inserts into the sodium dodecyl sulfate micelle primarily as a helix with a conserved glycine at the micelle–water interface, J. Virol. 71 (9) (1997) 6593–6602.
[35] D.G. Kneller, F.E. Cohen, R. Langridge, Improvements in protein secondary structure prediction by an enhanced neural network, J. Mol. Biol. 214 (1990) 171–182.
[36] D.G. Kneller, F.E. Cohen, R. Langridge, Improvements in protein secondary structure prediction by an enhanced neural network, J. Mol. Biol. 214 (1990) 171–182.
[37] C. Branden, J. Tooze, Introduction to Protein Structure, Garland, New York, 1998.

[38] L. Tortech, C. Jaxel, M. Vincent, J. Gallay, B. de Foresta, The polar headgroup of the detergent governs the accessibility to water of tryptophan octyl ester in host micelles, BBA-Biomembr. 1514 (1) (2001) 76–86.
[39] T. Imamura, K. Konishi, Interaction of indole and tryptophan derivatives with sodium dodecyl sulfate micelles measured with ultraviolet absorption and fluorescence quenching, J. Protein Chem. 14 (1995) 409–417.
[40] J. Ren, S. Lew, Z. Wang, E. London, Transmembrane orientation of hydrophobic alpha helices is regulated both by the relationship of helix length to bilayer thickness and by cholesterol concentration, Biochemistry 36 (1997) 10213–10220.
[41] T. Imamura, K. Konishi, Interaction of tryptophan dipeptides with sodium dodecyl sulfate micelles, J. Collloid and Interace Sci. 198 (1998) 300–307.
[42] Y. Chen, M.D. Barkley, Toward understanding tryptophan fluorescence in proteins, Biochemistry 37 (28) (1998) 9976–9982.
[43] K.A. Riske, O.R. Nascimento, M. Peric, B.L. Bales, M.T. Lamy-Freund, Probing DMPG vesicle surface with a cationic aqueous soluble spin label, Biochim. Biophys. Acta 1418 (1999) 133–146.
[44] C.-H. Hsu, S.-H. Wu, D.-K. Chang, C. Chen, Structural characterizations of fusion peptide analogs of influenza virus hemagglutinin, J. Biol. Chem. 277 (2002) 22725–22733.
[45] A.M. Dixon, R.M. Venable, R.W. Pastor, T.E. Bull, Micelle-bound conformation of a hairpin-forming peptide: combined NMR and molecular dynamics study, Biopolymers 65 (2002) 284–298.